

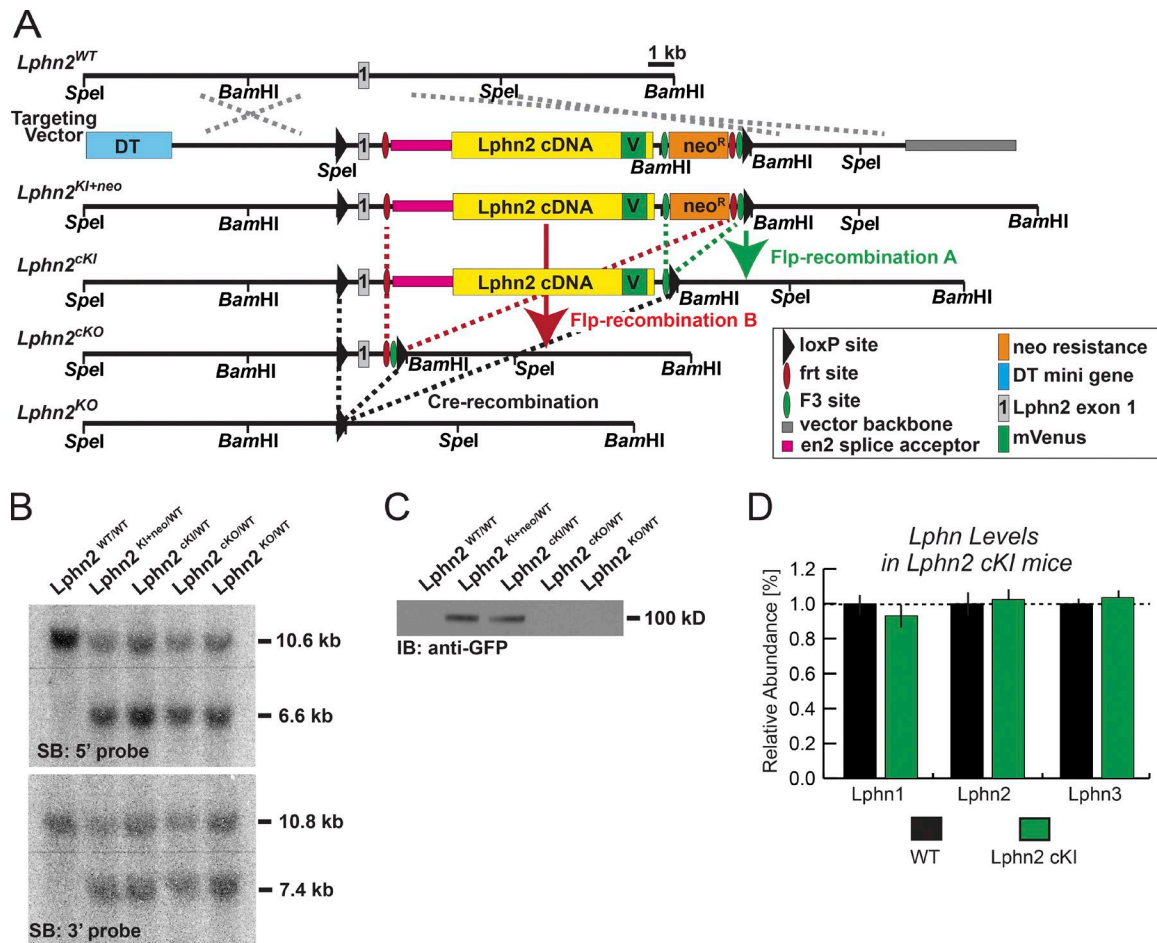
Anderson et al., <https://doi.org/10.1083/jcb.201703042>

Figure S1. **Strategy for the generation and validation of *Lphn2* mutant mice.** (A) Schematic of the *Lphn2* gene (*Adgrl2*)-targeting strategy. In the intron downstream of exon 1 containing the *Lphn2* start codon and signal peptide, sequences were inserted that (a) included an artificial exon encoding a full-length *Lphn2*-mVenus fusion protein minus the signal peptide (mVenus was positioned after residue 1,131) and (b) a neomycin resistance selection cassette. Two pairs of distinct Flp recombination sites (red, frt; green, F3) allow removal of the neomycin cassette with generation of either a *Lphn2* cKI allele (*Lphn2*<sup>cKI</sup>) or a *Lphn2* cKO (*Lphn2*<sup>cKO</sup>) allele. loxP sites (arrowheads) flank the 5' coding sequences in both alleles to allow Cre recombinase-mediated deletion of the cKI or cKO genotypes. DT, diphtheria toxin selection cassette. (B) Southern blot (SB) analyses using 5' and 3' outside probes were performed to verify initial proper homologous recombination as well as Flp- and Cre recombinase-mediated recombination events in different *Lphn2* alleles. (C) Immunoblotting (IB) of whole-brain lysates using GFP antibodies detected *Lphn2* mVenus protein in mice carrying the *Lphn2*-mVenus cKI alleles (*Lphn2*<sup>cKI+neo</sup> and *Lphn2*<sup>cKI</sup>). Because of cleavage of mature *Lphn2* protein at the GPCR proteolysis site, the immunosignal (~100 kD) represents the C-terminal fragment of the *Lphn2*-mVenus protein. (D) Quantitative RT-PCR analysis of brain RNA to determine relative mRNA levels of *Lphn1*, *Lphn2*, and *Lphn3* in homozygous WT and *Lphn2* cKI mice. Data are means  $\pm$  SEM ( $n = 4$ ).

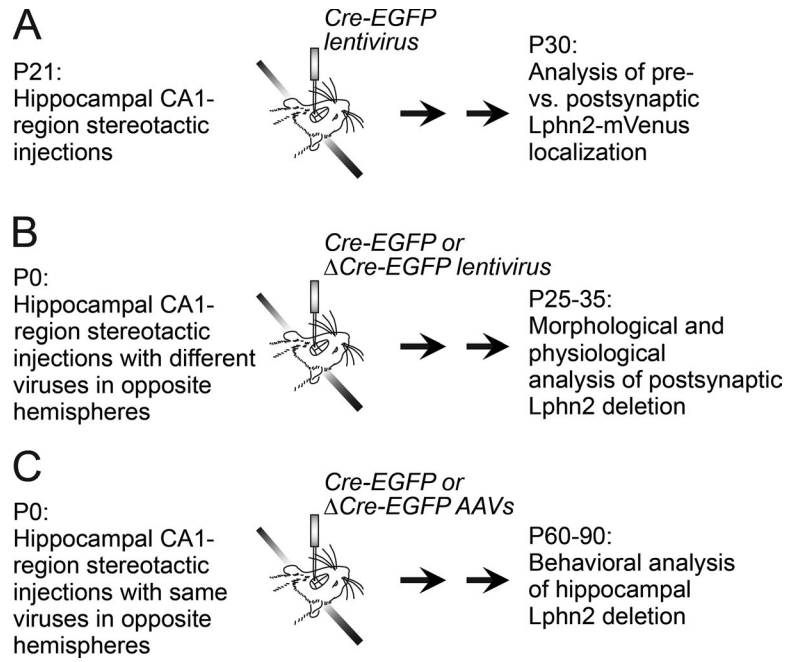


Figure S2. **Experimental strategies used for stereotactic injections of viruses into the hippocampal CA1 region.** (A) Experimental design for stereotactic injection of lentiviruses expressing EGFP–Cre recombinase into the CA1 region of Lphn2-mVenus cKI mice to test whether Lphn2-mVenus is pre- or postsynaptic in the SLM (Fig. 2, F and G). (B) Experimental design for stereotactic injection of lentiviruses expressing mutant ( $\Delta$ Cre) or WT EGFP–Cre recombinase into the CA1 region of newborn (P0) Lphn2 cKO mice to test whether the Lphn2 alters spine density and/or synaptic transmission (Fig. 2, H and I; and Fig. 3). (C) Experimental design for stereotactic injection of AAVs expressing mutant ( $\Delta$ Cre) or WT EGFP–Cre recombinase into the CA1 region of newborn (P0) Lphn2 cKO mice to test animal behavior (Fig. 4).

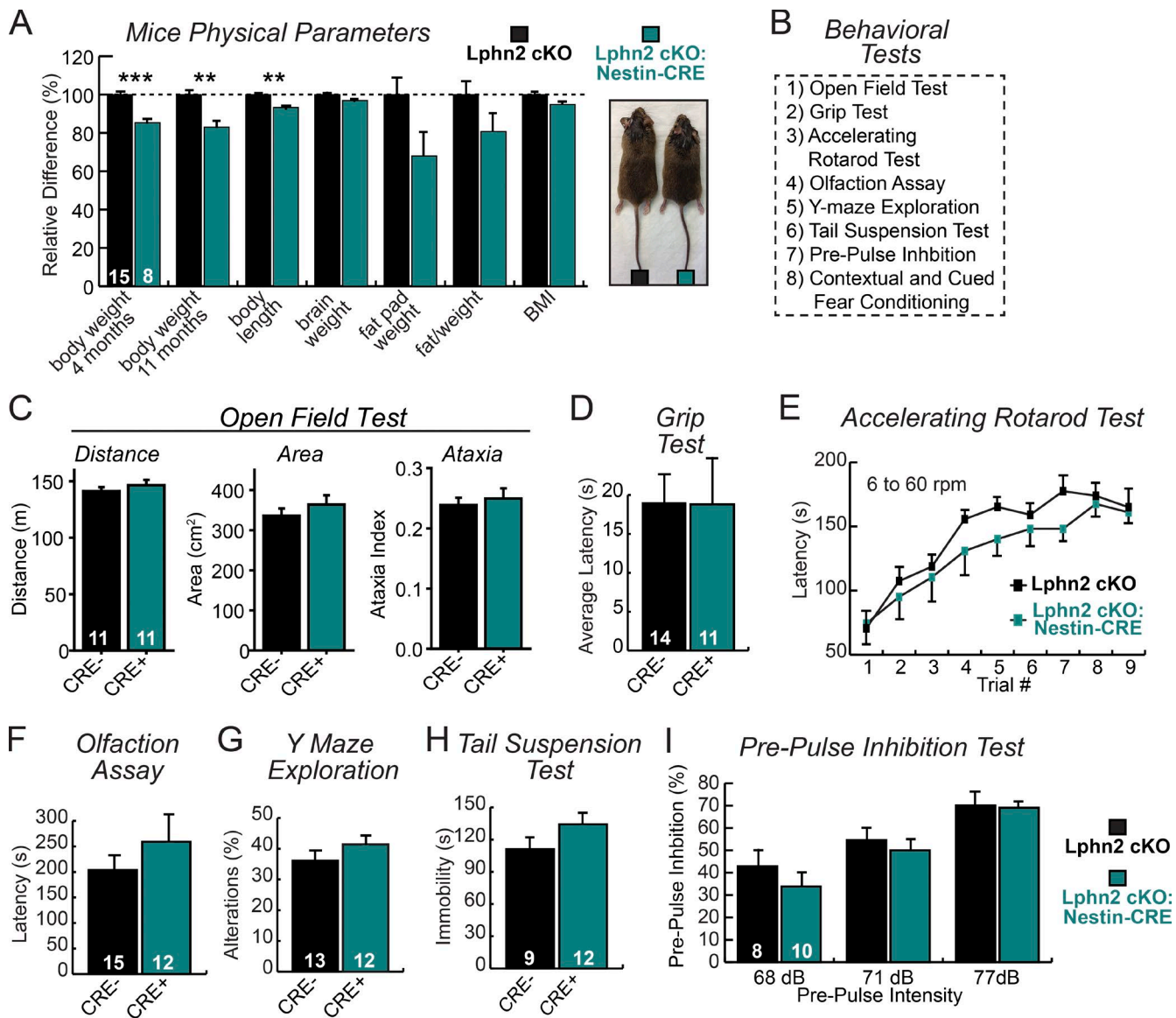


Figure S3. **Further analysis of the brain-specific deletion of Lphn2 mediated by crossing Nestin-Cre mice with Lphn2 cKO mice.** (A) Homozygous female Lphn2 cKO mice were crossed to male Lphn2 cKO mice containing a single Nestin-Cre allele to generate offspring that were homozygous for Lphn2 cKO and either negative (CRE-) or positive (CRE+) for the Nestin-Cre transgene. The various parameters shown were analyzed in littermate mice at 11 mo of age except for the body weight, which was examined at both 4 and 11 mo at age. BMI, body mass index. Data shown are normalized for littermate controls. (B) Sequence of behavioral tests performed in littermate Lphn2 cKO mice with and without Nestin-Cre expression. (C) Summary graphs of open field tests performed on a force-plate actometer during a 30-min session, measuring distance traveled (left), exploration area (middle), and ataxia index (right). (D) Mean three-trial latency fell from an inverted wire mesh during the grip test. (E) Latency to fall from an accelerating rotarod during nine trials across 3 d (three trials per day). (F) Latency to retrieve a hidden food pellet during the olfaction assay. (G) Spontaneous alterations during exploration in the Y-maze (in percentages). (H) Time spent immobile during 6 min of the tail suspension test. (I) Prepulse inhibition of the acoustic startle response. The percent inhibition of the startle response was calculated for three prepulse intensities (68, 71, and 77 dB) preceding a 115-dB tone. Data are means  $\pm$  SEM. Numbers of mice examined are shown in the bars for each set of experiments. Statistical analyses were performed using Student's *t* test. \*\*,  $P < 0.01$ ; \*\*\*,  $P < 0.001$ .

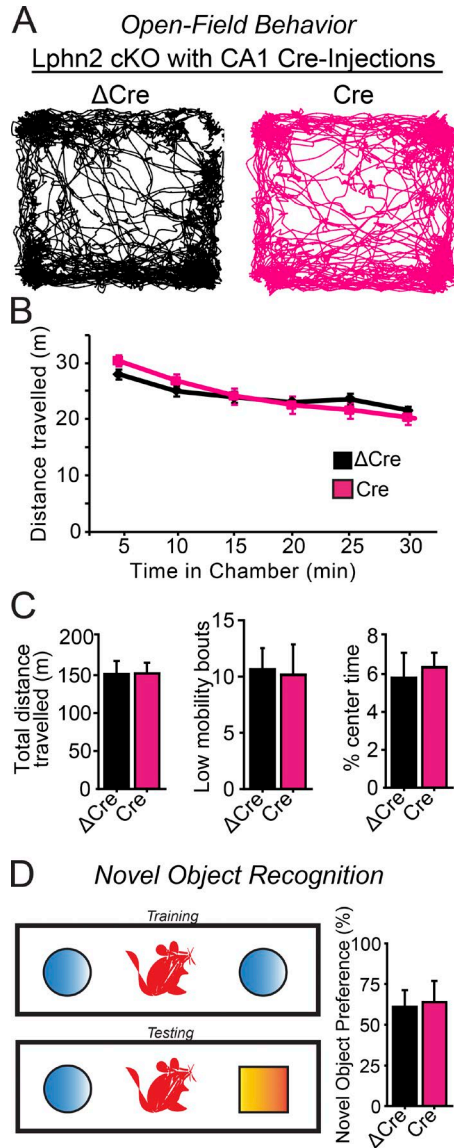


Figure S4. **Deletion of Lphn2 by stereotactic delivery of AAV-Cre viruses into the CA1 region of the hippocampus does not alter open field or novel object recognition behaviors.** (A) Representative activity traces of mice in the open-field arena as monitored on a force plane. AAVs expressing inactive ( $\Delta$ Cre; control) or active Cre recombinase were bilaterally injected into the CA1 region of Lphn2 cKO mice at birth, and mice were analyzed behaviorally at 2–3 mo of age. (B) Summary plot of total distance traveled in the open-field assay, plotted in 5-min bins during the course of a 30-min trial ( $n = 10$   $\Delta$ Cre–; 11 Cre-injected mice). (C) Summary graphs of the total distance traveled, low-mobility bouts, and percentage of time spent in the center of the open field during a 30-min open-field assay. Low-mobility bouts were defined as inactivity for a total of  $\geq 5$  s. Percent center time was defined as the fraction of time spent in the central 25% area of the open-field chamber ( $n =$  same as B). (D) Outline of novel object recognition assay (left) and summary graph of the novel object preference measured in the assay (right). Mice explored two identical objects in a chamber during two training trials. One object was subsequently changed to a new object during the test trial, and the percent time spent exploring the novel object was measured as plotted in the summary graph ( $n =$  same as B). Summary data are means  $\pm$  SEM.